Stability Enhancement of Wind Farm Connected Power System Using Superconducting Magnetic Energy Storage Unit

Arghya Mitra
Dept. of Electrical Engineering
Indian Institute of Technology Kharagpur
Kharagpur, India
mitrarghya@gmail.com

Dheeman Chatterjee
Dept. of Electrical Engineering
Indian Institute of Technology Kharagpur
Kharagpur, India
dheemanc@gmail.com

***Abstract*— This paper deals with the enhancement of the transient stability of the power system integrated with Doubly Fed Induction Generator (DFIG) based wind farms connected with Superconducting Magnetic Energy Storage (SMES) unit. The fluctuation in the wind power injection to the system due to variability in wind speed can also be reduced by the introduction of the SMES unit. The study is carried out in SMIB system and WSCC 3-machine 9-bus system in PSCAD/EMTDC platform.**

Keywords*— *Transient Stability; Power System; DFIG; SMES;

I. INTRODUCTION

With the increase in the environmental impacts on the society due to the use of fossil fuel based power plants, the use of renewable power as an alternate source of energy raises rapidly. Wind due to its easy availability is one of the major sources of alternate energy. Because of certain advantages the variable speed DFIG based wind farms are gaining popularity over fixed speed squirrel cage induction generator (SCIG) based wind farms. DFIG based wind farms can operate in both sub-synchronous and super-synchronous speed regimes extracting maximum power from wind [1].

There is a fluctuation of output power of the wind farm because of the intermittent and variable nature of the wind. So, when the wind power plant is integrated with the grid the fluctuation in generated power affect the power system stability. An energy storage unit can reduce the net fluctuation in injected power to the grid. Research is going on the different kind of energy storage units that can be used to improve the power quality and stability of the system [2, 3]. The energy storage units can be listed as Super Capacitor Energy Storage (SCES), Compressed Air Energy Storage system (CAESS), Fly Wheel Energy Storage System (FESS), Pumped Hydro Energy Storage System (PHESS), Battery Energy Storage System (BESS) and Superconducting Magnetic Energy Storage (SMES). Among all SMES unit is very popular while considered to be connected with wind farm because of its high efficiency, high capacity and a very fast response with respect to the other [3]. SCES has also high efficiency and capacity but SMES has very long life time in comparison to SCES. BESS is also used as an energy storage unit in connection with wind farm but it has a limited life cycle along with its voltage and current limitations [4]. SMES is a large superconducting coil. It is capable of storing electric energy in the magnetic field generated by dc current flowing through the coil [5]. An application of SMES unit to improve the DFIG power dispatch and dynamic performance during intermittent misfire and fire-through faults is seen in [6]. Again application of SMES to enhance the dynamic performance of DFIG during voltage sag and swell is investigated in [7]. Application of SMES is also seen in wind farm to improve the voltage stability [8]. The transient stability enhancement of SCIG based wind farm is seen in [9-11]. The energy capacitor system is used in [12] to improve the transient stability of a multi-machine power system which includes SCIG based wind farm.

Here the SMES unit is used to enhance the transient stability of the power system integrated with DFIG based wind farm. The SMES unit can also be able to reduce the fluctuation in power output of the wind farm due to variation in wind speed. The study is carried out in PSCAD/EMTDC simulator and the systems used for the study are single machine infinite bus system (SMIB) and WSCC 3-machine 9-bus system.

II. MODELLING OF POWER SYSTEM, DFIG AND SMES

A. Modeling of synchronous machine and the network

The flux decay model of synchronous machine is considered along with a static exciter of one gain and one time constant [13, 14]. The transmission lines are

978-1-4799-5141-3/14/$31.00

represented by equivalent π structure. The loads are considered to be of constant impedance type.

B. Modelling of the DFIG and its controller

The wind turbine and the DFIG rotating mass is represented by a two mass model [15, 16]. The mechanical torque of the wind turbine is a function of wind velocity [15-17]. The stator and the rotor circuits of DFIG are represented by their respective differential equations for a balanced and unsaturated condition [15, 16].

The connection diagram of DFIG along with SMES to the load bus of a power system is as shown in Fig. 1. The DFIG is connected through a double circuit line and a transformer [18] to a load bus of the existing power system as shown in Fig. 1. The SMES unit is also connected to the same load bus through a transformer.

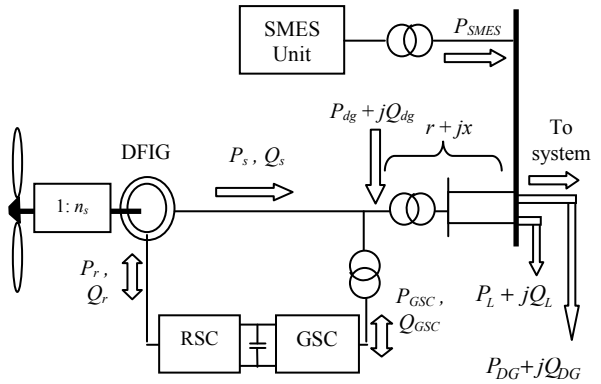

Fig. 1. Connection of DFIG and SMES to the system load bus

In Fig. 1, n_s is the gear box ratio, r and x are resistance and reactance of the line connecting the DFIG to the system. RSC stands for rotor side converter and GSC stands for grid side converter. The load connected to the system bus in the original system (without DFIG) is ($P_L + jQ_L$). An additional load of ($P_{DG}+ jQ_{DG}$) is assumed to be connected to the bus as shown in Fig. 1 [19, 20]. Under rated wind speed, the DFIG would supply this additional load as well as the losses in the connecting transformer and line, while the steady state power flow in the original network remains same.

Total active and reactive powers delivered to the grid by DFIG are

$$P_{dg} = P_s + P_r = V_{ds} i_{ds} + V_{qs} i_{qs} + V_{dr} i_{dr} + V_{qr} i_{qr} \quad (1)$$

$$Q_{dg} = Q_s + Q_{GSC} = V_{qs} i_{ds} - V_{ds} i_{qs} \quad (2)$$

Here, P_s and Q_s are the stator active and reactive powers. P_r is rotor active power, V_{ds}, V_{qs}, V_{dr}, and V_{qr} are the stator and the rotor d-axis and q-axis voltages respectively, i_{ds} and i_{qs} are the stator d-axis and q-axis currents, i_{dr}, and i_{qr} are the rotor d-axis and q-axis currents respectively. GSC is operated at unity power factor making its reactive power (Q_{GSC}) equal to zero.

In this work, the d-axis of the synchronously rotating reference frame is considered to be oriented along the stator voltage V and the q-axis is leading the d-axis, hence

$$V_{ds} = V \text{ and } V_{qs} = 0 \quad (3)$$

$$\psi_{ds} \cong 0 \text{ and } \psi_{qs} \cong \psi_s \quad (4)$$

Here, ψ_{ds} and ψ_{qs} are the stator d-axis and q-axis flux, ψ_s is the stator flux. The electromagnetic torque thus can be expressed as

$$T_e = -\left(L_m / L_{ss}\right) \psi_{qs} i_{dr} \quad (5)$$

Similarly, the stator reactive power can be expressed as a function of q-axis rotor current i_{qr} as

$$Q_s = \left(L_m V_{ds} / L_{ss}\right) i_{qr} - \left(V_{ds} \psi_{qs} / L_{ss}\right) \quad (6)$$

Where, L_m is the mutual inductance, L_{ss} and L_{rr} are stator and rotor inductances. It can be seen from (5) and (6) that the T_e and Q_s can be separately controlled by i_{dr} and i_{qr} respectively. Using these relations, the normal field oriented control [1] of the RSC of the DFIG becomes as shown in Figure 2(a) and 2(b).

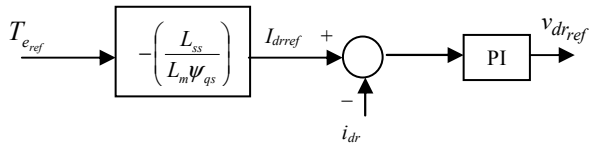

Fig. 2(a). d-axis control block

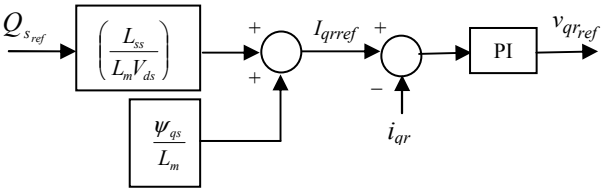

Fig. 2(b). q-axis control block

In Figure 2(a) $T_{e_{ref}}$ is the reference torque and is obtained by

$$T_{e_{ref}} = K_{opt}\, \omega_r^2 \quad if \quad \omega_r < \omega_{r_{rated}}$$
$$= T_{e_{rated}} \quad if \quad \omega_r \geq \omega_{r_{rated}} \quad (7)$$

Where K_{opt} in pu is given by [15]

$$K_{opt} = 0.5 \rho \pi R^5 C_{p\max} \omega_{tB}^2 / \left(\lambda_{opt}^3 S_B\right) \quad (8)$$

Here $T_{e_{rated}}$ stands for the rated torque, ω_r is the per unit rotor speed, $\omega_{r_{rated}}$ is the per unit rated DFIG speed, C_{pmax} is the maximum coefficient of performance; λ_{opt} is optimum tip speed ratio, R is the wind turbine blade length, ρ is the air density, S_B and ω_{tB} are the base power and the base speed of the wind turbine respectively. The amount of reactive power to be supplied by the DFIG is set as the stator reactive power

reference ($Q_{s_{ref}}$).

Rearrangement of (5) and (6) gives the expressions of the references of the *d*-axis and *q*-axis rotor currents

$$I_{drref} = -\left(L_{ss}/L_m\psi_{qs}\right)T_{e_{ref}} \quad (9)$$

$$I_{qrref} = \left(L_{ss}/L_m V_{ds}\right)Q_{s_{ref}} + \left(\psi_{qs}/L_m\right) \quad (10)$$

I_{drref} is compared with the actual rotor current and the error signal is passed through a P-I controller to generate the rotor *d*-axis voltage reference ($v_{dr_{ref}}$).

Similarly using a P-I controller *q*-axis rotor voltage reference ($v_{qr_{ref}}$) can be generated from I_{qrref}. Now, *d*-*q*-0 to *a*-*b*-*c* transformation on $v_{dr_{ref}}$ and $v_{qr_{ref}}$ gives the phase voltage references. These are then used as the modulating signals in PWM to generate the switching pulses for RSC. Similar to RSC, the stator voltage orientation is considered for the control structure of GSC also for the decoupled control of active and reactive power flowing through the converter. By maintaining the DC bus voltage constant it is ensured that the GSC allows bi-directional flow of active power between the grid and the RSC. The reactive power flow is controlled such that the GSC is operated at unity power factor.

The pitch controller of the wind turbine increases the turbine blade pitch angle to reduce the mechanical power whenever the wind speed (thus ω_r) exceeds the rated value, to keep DFIG active power output constant at its rated value.

To provide fault ride through capability, the rotor of the DFIG is short circuited during fault through crowbar (an external resistance), thus making the DFIG acts like a singly excited machine. For a realistic simulation, the crowbar is made active after a 5 ms delay of the occurrence of the fault and is made inactive (by removing the crowbar) after a similar time delay when the fault is cleared. The converter is out of the circuit when the crowbar is connected.

C. Modelling of the SMES and its controller

The SMES unit used in this work consists of a superconducting coil (*L*), a voltage source converter (VSC), a DC link capacitor (C_{DC}) and a two quadrant DC-DC chopper as shown in Fig. 3 [4-6]. The SMES unit is then connected through a transformer to the system grid.

The VSC provides a power electronic interface between AC power system and the superconducting coil. The DC link voltage across C_{DC} is maintained constant by the VSC.

The control structure of it is same as that of the

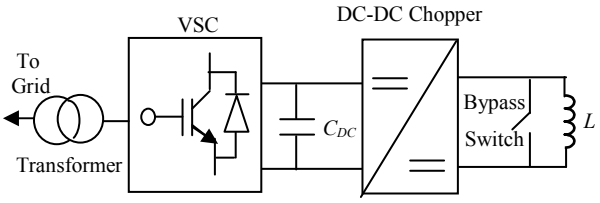

Fig. 3. VSC based SMES with a DC-DC chopper

GSC of the DFIG. The superconducting coil is charged or discharged by a two quadrant DC-DC chopper. The DC-DC chopper is controlled the voltage across the SMES coil (positive or negative) and the stored energy can then be charged or discharged. The duty cycle of PWM operation to reduce the wind generator output power fluctuations as an effect of the wind speed variability is decided by a PI controller. The control structure of the chopper is as shown in the Fig. 4. The duty cycle (*D*) determines the direction and magnitude of power exchange between the SMES coil and the AC system as presented in Table I.

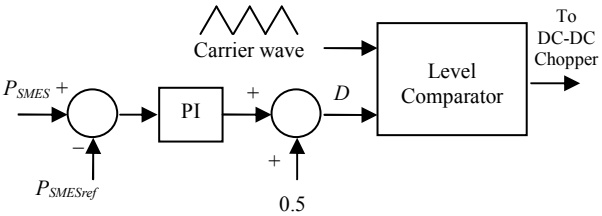

Fig. 4. Control structure DC-DC chopper

TABLE I
DUTY CYCLE RULES

D	SMES coil action
$D = 0.5$	Standby
$0.5 < D \leq 1$	Charging
$0 \leq D < 0.5$	Discharging

If *D* is equal to 0.5, no action will be taken by the superconducting coil. In this condition, a bypass switch across the SMES coil (shown in Fig. 3) will be closed to avoid the discharging of SMES. The bypass switch is controlled in such a way that it will be closed if *D* is equal to 0.5 otherwise it will be opened. When the grid power decreases, *D* will reduce accordingly to be in the range of 0 to 0.5. The stored energy in the SMES coil will be transferred to the AC system during this time. Charging of the SMES coil takes place when *D* is in the range of 0.5 to 1.0.

The relation between V_{SMES} and $V_{DC,SMES}$ can be written as [21]:

$$V_{SMES} = (1 - 2D)V_{DC\_SMES} \quad (11)$$

Where,
V_{SMES} is the average voltage across the SMES coil
D is duty cycle
V_{DC_SMES} is the average voltage across the DC link capacitor

During fault the SMES is deliberately made to operate in charging mode irrespective of the value of the duty cycle so that the overall system stability increases due to increase in the demand of the system.

III. Simulation Result

The study is carried out on SMIB system [22] and WSCC 3-machine 9-bus system [13] in PSCAD/EMTDC platform. The critical clearing is compared for the cases with and without SMES connected to the power system integrated with a wind farm. The results are taken for constant as well as variable wind speed.

A. Result for SMIB system

The SMIB system connected with a wind farm is shown in the Fig. 5. The SMIB system is modified by introducing two load buses (Bus 4 and bus 5). Wind farm, of a capacity of 200 MW (40 units of 5 MW each [16]), is connected to one of the load buses (Bus 4). An aggregated model of the wind farm is considered. The rating of SMES unit is 60 MW, 750 MJ.

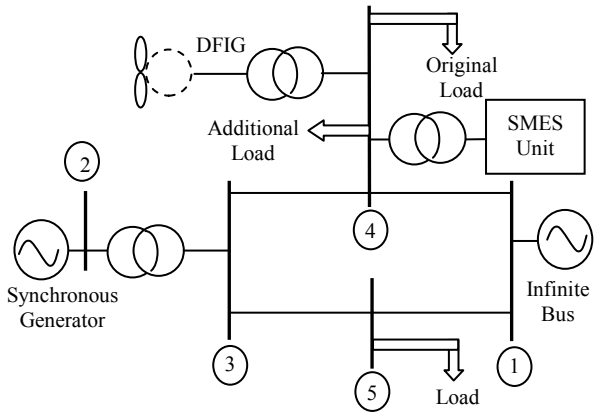

Fig. 5. Schematic diagram of the SMIB system with wind farm and SMES

The wind speed (V_w) is considered to be variable following a profile [23] as shown in Fig. 6 (a 50 s window). Study is carried out to observe the effectiveness of the SMES unit to maintain the wind power injected to the grid (P_g) at nearly constant value under this variable wind speed condition.

Fig. 7 shows the variation of P_g with and without SMES in the system. It is observed that in presence of the SMES the variation in the power injected to the grid decreases even in the case of a very high wind speed variation.

The stability enhancement is studied first with constant wind speed (V_w) at 14.75 m/s (close to its rated speed of 15 m/s). At this wind speed, the wind farm will generate 190 MW. The 3-phase short circuit self-clearing fault is considered at two different buses viz.

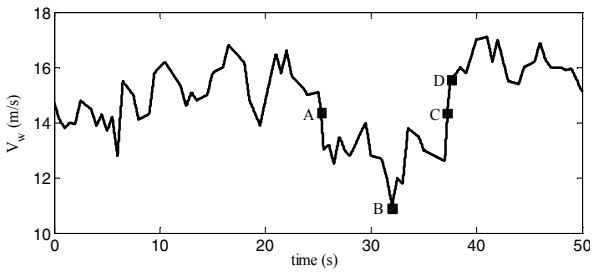

Fig. 6. Wind profile

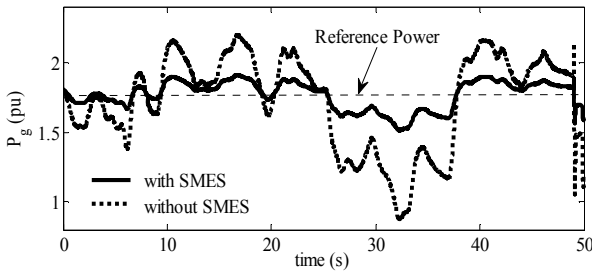

Fig. 7. Variation in P_g with and without the presence of SMES

synchronous generator terminal bus (bus 3) and one of the load buses (Bus 5). The critical clearing time (t_{cr}) is calculated for these two cases first without SMES in the system and then t_{cr} is calculated for the same cases now with SMES in the system.

Fig. 8 shows the variation of relative delta (δ) of the alternator at a fault clearing time of 472 ms. The plot of δ (dotted line) becomes unbounded in absence of SMES indicating an unstable system while the system becomes stable (bounded δ) when SMES is introduced in the system (continuous line).

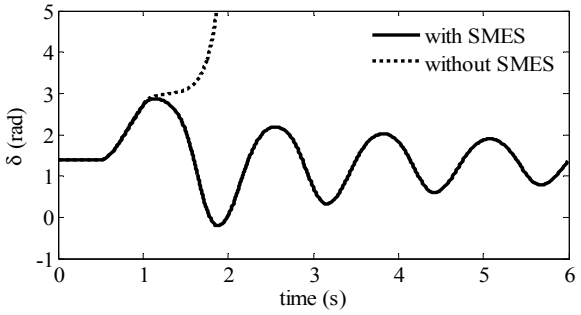

Fig. 8. Alternator relative rotor angle variation for a fault at bus 5

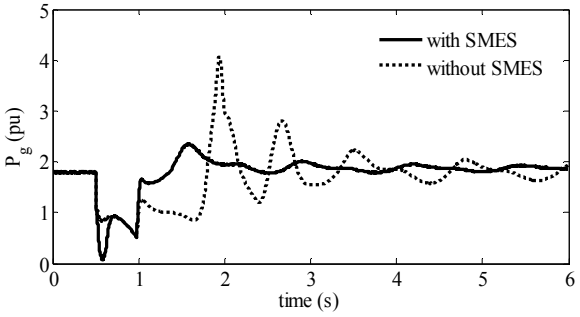

Fig. 9. Power injected to grid for a fault at bus 5

Fig. 9 shows the variation of P_g for the same condition both with and without SMES in the system. The comparisons of the t_{cr} with and without SMES for these two fault locations are shown in Table II.

With a variable wind speed, the instant of the occurrence of the fault makes some difference in system condition as the wind speed and its gradient differs, as shown by points A, B, C and D on the wind profile of Figure 6. Study is carried out considering these five points (one at a time) as the fault occurrence instant. The corresponding wind speeds are V_{wA}, V_{wB}, V_{wC}, and V_{wD}. At points A and C the corresponding wind speeds have same value but one has a downward direction (at A) and other has an upward directions. The wind speeds V_{wB}, V_{wC} and V_{wD} have upwards directions. Again V_{wB} is corresponding to minimum wind speed along the profile. At D wind speed is greater than the rated speed of 15 m/s. The comparisons of the t_{cr} with and without SMES at these four instants are also shown in Table II. It is seen from the Table II that with the introduction of SMES t_{cr} always increases both with constant and variable wind speed.

TABLE II
COMPARISON OF t_{cr}

Constant wind speed at 14.75 m/s					
DFIG at (Bus)	Fault at (Bus)		t_{cr} without SMES (ms)	t_{cr} with SMES (ms)	Improve-ment (ms)
4	3		236	246	10
	5		471	485	14
Variable wind speed					
DFIG at (Bus)	Fault at (Bus)	V_w (m/s)	t_{cr} without SMES (ms)	t_{cr} with SMES (ms)	Improve-ment (ms)
4	3	V_{wA} = 14.5	236	249	13
		V_{wB} = 11.0	246	251	5
		V_{wC} = 14.5	246	254	8
		V_{wD} = 15.5	236	247	11
	5	V_{wA} = 14.5	464	482	18
		V_{wB} = 11.0	489	499	10
		V_{wC} = 14.5	481	490	9
		V_{wD} = 15.5	467	479	12

B. Result for 3-machine 9-bus system

An aggregated wind farm model of capacity 100 MW (20 units of rating 5 MW each) is integrated with the WSCC 3-machine, 9-bus system as shown in Fig. 10. The disturbance considered is a 3-phase short-circuit fault in one of the load buses. The rating of SMES unit is 30 MW, 570 MJ.

The t_{cr} for a fault at bus 5 at point 'D' on the wind profile without SMES is 391 ms, so the system becomes unstable with fault clearing time of 391 ms as can be seen in Fig. 11 (dotted line with unbounded δ_{21}). For the same condition the system becomes stable with bounded δ_{21} when SMES is connected to the system

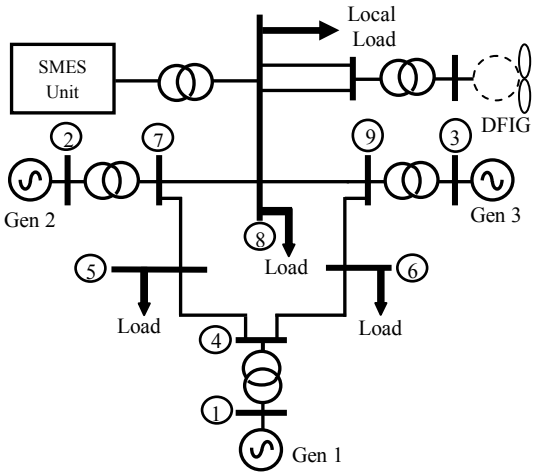

Fig. 10. WSCC 3-machine 9-bus system with DFIG and SMES connected to bus 8.

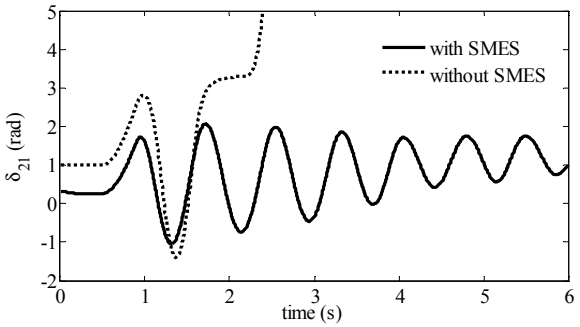

Fig. 11. Alternator relative rotor angle variation for a fault at bus 5

(continuous line in Fig. 11). The levels of δ for the two cases before the fault are slightly different as due to the introduction of the SMES the steady state power level changes. The t_{cr} in this case increases to 524 ms (Table III).

For the above condition the plots of DFIG electromagnetic torque (T_e) both with SMES and without SMES are shown in Fig. 12. As the system becomes unstable with a fault clearing time of 391 ms at an instant 'D' when SMES is absent, T_e shows an unstable nature along the time axis (dotted line), whereas a steady nature of T_e (continuous line) is visible because of a stable system condition when SMES is present in the system.

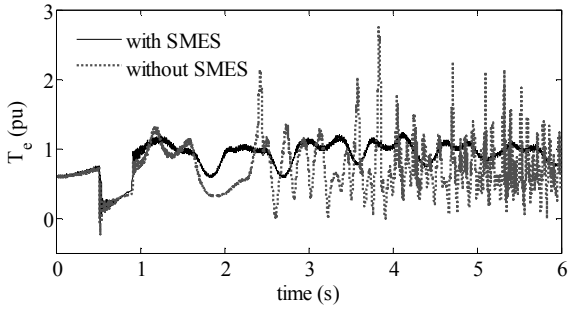

Fig. 11. DFIG electromagnetic torque variation for a fault at bus 5

Table III shows the comparison of t_{cr} for 9-bus system both for constant and variable wind speed conditions for two different fault locations of bus 5 and bus 6 with wind farm and SMES at bus 8. The last column of Table III shows the improvement in stability of the power system in terms of t_{cr}. As in SMIB system here also it is seen that there is an improvement of transient stability when SMES is connected and properly controlled.

TABLE III
COMPARISON OF t_{cr}

Constant wind speed at 13.95 m/s				
DFIG at (Bus)	Fault at (Bus)	t_{cr} without SMES (ms)	t_{cr} with SMES (ms)	Improve-ment (ms)
8	5	0.475	0.489	14 ms
	6	0.536	0.572	36 ms

Variable wind speed					
DFIG at (Bus)	Fault at (Bus)	V_w (m/s)	t_{cr} without SMES (ms)	t_{cr} with SMES (ms)	Improve-ment (ms)
8	5	V_{wA} = 14.5	0.112	0.235	123 ms
		V_{wB} =11.0	0.309	0.405	96 ms
		V_{wC} =14.5	0.400	0.569	169 ms
		V_{wD} =15.5	0.390	0.524	134 ms
	6	V_{wA} = 14.5	0.123	0.256	133 ms
		V_{wB} =11.0	0.305	0.396	91 ms
		V_{wC} =14.5	0.418	0.675	257 ms
		V_{wD} =15.5	0.408	0.583	175 ms

IV. CONCLUSION

This paper deals with the enhancement of the transient stability of power system connected with a wind farm when SMES unit is introduced in the system. The study shows that there is always an improvement in the stability in terms of the critical clearing time in presence of SMES unit both for constant and variable wind speed conditions. The systems considered for the study are single machine infinite bus system and WSCC 3-machine 9-bus system and the study is carried out in PSCAD/EMTDC simulator.

REFERENCES

[1] M. V. A. Nunes, J. A. P. Lopes, H. H. Zurn, U. H. Bezerra and R. G. Almeida, "Influence of the variable-speed wind generators in transient stability margin of the conventional generators integrated in electrical grids," IEEE Trans. on Energy Conversion, vol. 19, no. 4, December 2004, pp. 692-701.

[2] S. C. Smith, P. K. Sen and B. Kroposki, "Advancement of energy storage devices and application in electrical power system," Power and Energy Society General Meeting - Conversion and Delivery of Electrical Energy in the 21st Century, 2008 IEEE , 20-24 July 2008, pp. 1-8.

[3] R. Gupta et al, "Application of energy storage devices in power system," International Journal of Engineering, Science and Technology vol. 3, no. 1, 2011, pp. 289-297.

[4] Mohd. H. Ali, B. Wu, R. A., Dougal, "An overview of SMES applications in power and energy systems," IEEE Trans. on Sustainable Energy, vol.1, no.1, April 2010, pp. 38-47.

[5] W. Buckles and W. Hassenzahl, "Superconducting magnetic energy storage," IEEE Power Eng. Rev., vol. 20, no. 5, May 2000, pp. 16–20.

[6] A. M. S. Yunus, , A. Abu-Siada, and M. A. S., Masoum, "Application of SMES unit to improve DFIG power dispatch and dynamic performance during intermittent misfire and fire-through faults," IEEE Trans. on Applied Superconductivity, vol.23, no.4, Aug. 2013, pp. 5701712-5701712.

[7] A. M. S. Yunus, , M. A. S. Masoum and A. Abu-Siada, "Application of SMES to enhance the dynamic performance of DFIG during voltage sag and swell," IEEE Trans. on Applied Superconductivity, vol.22, no. 4, Aug. 2012, pp. 5702009-5702017.

[8] J. Shi, Y.J. Tang, L. Ren, J.D. Li and S.J. Chen, "Application of SMES in wind farm to improve voltage stability," Physica C: Superconductivity, vol. 468, issues 15-20, September 2008, pp. 2100–2103.

[9] Mohd. H. Ali, M. Park, In-Keun Yu, T. Murata and J. Tamura, "Improvement of wind-generator stability by fuzzy-logic-controlled SMES," IEEE Trans. on Industry Applications, vol. 45, no. 3, May/June 2009, pp. 1045-1051.

[10] S. S. Chen, L. Wang, Z. Chen and Wei-Jen Lee, "Power-flow control and transient-stability enhancement of a large-scale wind power generation system using a superconducting magnetic energy storage (SMES) unit," Power and Energy Society General Meeting, 2008 IEEE , 20-24 July 2008, pp.1-6.

[11] M. R. I. Sheikh, S. M. Muyeen, R. Takahashi, T. Murata and J. Tamura, "Transient stability enhancement of wind generator using superconducting magnetic energy storage unit," 18th International Conference on Electrical Machines, 2008 (ICEM), 6-9 Sept. 2008, pp. 1-6.

[12] S. M. Muyeen, R. Takahashi, Mohd. H. Ali, T. Murata and J. Tamura, "Transient stability augmentation of power system including wind farm by using ECS," IEEE Trans. on Power Systems, vol. 23, no. 3, August 2008, pp. 1179-1187.

[13] P. W. Sauer and M. A. Pai, "Power System Dynamics and Stability," Pearson Education Asia, First Indian Reprint, 2002.

[14] P. Kundur, "Power System Stability and Control," McGraw-Hill, New York, 1994.

[15] F. Mei and B. Pal, "Modal analysis of grid-connected doubly fed induction generators," IEEE Trans. on Energy Conversion, Vol. 22, No. 3, September 2007, pp. 728- 736.

[16] F. Mei, "Small signal modeling and analysis of doubly fed induction generators in wind power applications," Ph.D. Thesis 2007, Imperial College London, University of London.

[17] S. K. Salman and A. L. J. Teo, "Windmill modeling consideration and factors influencing the stability of a grid-connected wind power-based embedded generator," IEEE Trans. on Power Systems, Vol. 18, No. 2, May 2003, pp. 793-802.

[18] P. Ledesma and J. Usaola, "Doubly fed induction generator model for transient stability analysis," IEEE Trans. on Energy Conversion, Vol. 20, No. 2, June 2005, pp. 388-397.

[19] M. K. Donnelly, J. E. Dagle, D. J. Trudnowski, and G. J. Rogers, "Impacts of the distributed utility on transmission system stability," IEEE Trans. on Power Systems, Vol. 11, No. 2, May 1996, pp. 741-746.

[20] A. Mitra and D. Chatterjee, "A sensitivity based approach to assess the impacts of integration of variable speed wind farms on the transient stability of power systems", Renew. Energy, Vol. 60, December 2013, pp. 662-671.

[21] I. D. Hassan, R. M. Bucci, and K. T. Swe, "400 MW SMES power conditioning system development and simulation", IEEE Trans. on Power Electronics, vol. 8, July 1993, pp. 237-249.

[22] S. M., Brahma, "Distance relay with out-of-step blocking function using wavelet transform," IEEE Trans. on Power Delivery, vol. 22, no. 3, July 2007, pp. 1360-1366.

[23] R. Datta, "Rotor side control of grid-connected wound rotor induction machine and its application to wind power generation", PhD Thesis 2000, Indian Institute of Science, Bangalore.